AD-A047 079 MINNESOTA UNIV MINNEAPOLIS DEPT OF AEROSPACE ENGINE--ETC F/G 20/11
STRUCTURAL INELASTICITY XVIII. A SLIP MODEL FOR FINITE ELEMENT --ETC(U)
SEP 77 H VAN RIJ, P G HODGE N00014-75-C-0177
UNCLASSIFIED AEM-H1-18 NL

1 OF 1
ADA047 079

END
DATE FILMED
1-78
DDC

(14) Report AEM-H1-18

(6) STRUCTURAL INELASTICITY XVIII.

A Slip Model for Finite Element Plasticity.

(10) Hendrik van Rij, Research Assistant
Philip G. Hodge Jr., Professor of Mechanics
Department of Aerospace Engineering and Mechanics
University of Minnesota
Minneapolis, Minnesota 55455

(11) Sept. 1977

(12) 27 p.

(9) Technical Report.

(15) N00014-75-C-0177

Prepared for

OFFICE OF NAVAL RESEARCH
Arlington, VA 22217

OFFICE OF NAVAL RESEARCH
Chicago Branch Office
536 South Clark St.
Chicago, IL 60605

17-A042 767

405 395

SECURITY CLASSIFICATION OF THIS PAGE (When Data Entered)

REPORT DOCUMENTATION PAGE		READ INSTRUCTIONS BEFORE COMPLETING FORM
1. REPORT NUMBER AEM-H1-18 ✓	2. GOVT ACCESSION NO.	3. RECIPIENT'S CATALOG NUMBER
4. TITLE (and Subtitle) STRUCTURAL INELASTICITY XVIII A Slip Model for Finite Element Plasticity		5. TYPE OF REPORT & PERIOD COVERED Technical Report 6. PERFORMING ORG. REPORT NUMBER
7. AUTHOR(s) Hendrik van Rij, Research Assistant Philip G. Hodge, Jr., Professor of Mechanics		8. CONTRACT OR GRANT NUMBER(s) 000 N14-75-C-0177
9. PERFORMING ORGANIZATION NAME AND ADDRESS University of Minnesota Minneapolis, Minnesota 55455		10. PROGRAM ELEMENT, PROJECT, TASK AREA & WORK UNIT NUMBERS NR 064-429
11. CONTROLLING OFFICE NAME AND ADDRESS OFFICE OF NAVAL RESEARCH Arlington, VA 22217		12. REPORT DATE Sept. 1977 13. NUMBER OF PAGES 24
14. MONITORING AGENCY NAME & ADDRESS(if different from Controlling Office) OFFICE OF NAVAL RESEARCH Chicago Branch Office 536 South Clark St. Chicago, IL 60605		15. SECURITY CLASS. (of this report) Unclassified 15a. DECLASSIFICATION/DOWNGRADING SCHEDULE

16. DISTRIBUTION STATEMENT (of this Report)

Qualified requesters may obtain copies of this report from DDC

17. DISTRIBUTION STATEMENT (of the abstract entered in Block 20, if different from Report)

18. SUPPLEMENTARY NOTES

19. KEY WORDS (Continue on reverse side if necessary and identify by block number)

Plasticity, perfectly-plastic, finite element model, plain strain, notched bar, Prandtl punch

20. ABSTRACT (Continue on reverse side if necessary and identify by block number)

Conventional finite-element models are based on displacement or velocity fields which are at least continuous. However, it is known that perfectly plastic materials may exhibit discontinuities of the tangential velocity component along certain lines. In this investigation, a two-dimensional finite element model is proposed which will allow for such discontinuities.

A regular pattern of triangular elements is assumed.

(#20 con't on back page)

DD FORM 1 JAN 73 1473 EDITION OF 1 NOV 65 IS OBSOLETE
S/N 0102-014-6601

SECURITY CLASSIFICATION OF THIS PAGE (When Data Entered)

(number 20 con't)

The elements are assumed to be rigid and across the line separating any two adjoining elements the normal displacement component is continuous, but a discontinuity may exist in the tangential component. The defining equations-compatibility, equilibrium and constitutive-are developed with the aid of the Principle of Virtual Work.

Prandtl's punch problem is solved under plane strain conditions. Comparison is made with existing analytical and other numerical solutions, in order to evaluate the merits of allowing for discontinuities.

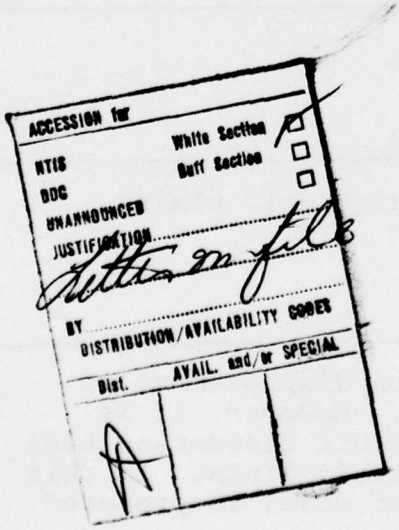

A SLIP MODEL FOR FINITE-ELEMENT PLASTICITY[1]

By

Hendrik van Rij[2]

and

Philip G. Hodge, Jr.[3]

Abstract

Conventional finite-element models are based on displacement or velocity fields which are at least continuous. However, it is known that perfectly plastic materials may exhibit discontinuities of the tangential velocity component along certain lines. In this investigation, a two-dimensional finite element model is proposed which will allow for such discontinuities.

A regular pattern of triangular elements is assumed. The elements are assumed to be rigid, and across the line separating any two adjoining elements the normal displacement component is continuous, but a discontinuity may exist in the tangential component. The defining equations - compatibility, equilibrium, and constitutive - are developed with the aid of the Principle of Virtual Work.

Prandtl's punch problem is solved under plane strain conditions. Comparison is made with existing analytical and other numerical solutions, in order to evaluate the merits of allowing for discontinuities

---

[1]This research was sponsored by the Office of Naval Research; the results are taken from a dissertation submitted to the University of Minnesota by one of the authors (H.v.R.) in partial fulfullment of the requirements for a Doctor of Philosophy degree.

[2]Engineer, Sichting Energieonderzoek Centrum Nederland, The Netherlands. Formerly Research Assistant, University of Minnesota

[3]Professor of Mechanics, University of Minnesota

1. Introduction. The basic concept of the finite element method is that a given structure or continuum is modeled by a finite assemblage of individual components or elements. Within each element and in the reactions between the elements simplifying assumptions are made in the static, kinematic, or constitutive equations.

In a pioneering paper in 1956, Turner, Clough, Martin, and Topp [1] proposed a finite element model for two dimensional problems which we shall refer to as the classical model. The elements are triangles and the model has the following properties: the displacement field is linear in each triangle and continuous over the whole domain; the strain stress fields are constant in each triangle; if the given body and surface force field is approximated by concentrated forces acting only at the nodes, then these forces must be in equilibrium at each node. The method has been extended to include plastic behavior.

Since the classical model and the slip model proposed herein are each based on a field which is kinematically admissible for the original continuum, the results will satisfy any kinematic minimum principle for the material involved. In particular, for an elastic/perfectly-plastic material the model yield-point will be an upper bound on that

*Numbers in square brackets refer to items listed in the bibliography.

of the continuum [2]. However, as first pointed out by Nagtegaal, Parks, and Rice [3], this upper bound may be very poor or even infinite if the model does not allow for incompressible motions.

This constraint, $\dot{\varepsilon}_{kk} = 0$, is not easily satisfied. Indeed, in a large field of 4N triangles, there will be approximately 2N nodes and two degrees of freedom per node so that there is an average of one degree of freedom per triangle. Therefore, one incompressibility constraint per triangle will leave essentially no degrees of freedom in the total domain, regardless of the number of elements.

Nagtegaal et al resolved this dilemma by requiring the triangles to be grouped in quadrilaterals such as the squares in Fig. 1. It is easily shown that if three of the four triangles in a quadrilateral undergo any incompressible deformation, the fourth will necessarily satisfy $\dot{\varepsilon}_{kk} = 0$. Thus there are only 3N constraints, which leaves one degree of freedom for each four triangles.

The velocity field associated with the yield-point load of many continuum problems exhibits another phenomenon which is not well modelled by the classical finite element model, namely, discontinuity of certain tangential velocity components. For example, let us consider the identation of a semi-infinite domain by a rigid beam under conditions of plane strain. For the simple case of a rigid/perfectly plastic material, Prandtl [4 , 2] presented a yield-point incipient flow field (see Fig. 8b) which

involved part of the domain (the triangles) moving as rigid bodies, and part of it (the quarter circle) deforming with zero volume change. We observe that the deforming part of the material moves relative to the non-deforming part with a finite tangential velocity discontinuity across the boundary separating the regions.

Therefore, in view of the facts that any continuous finite element model has difficulty representing incompressible flow, and that tangential velocity discontinuities actually exist in continuum solutions, it appears worthwhile to investigate a finite element model which will allow for such discontinuities.

In this paper we present a slip model in which these discontinuities are the only permissible motion, i.e. we consider an array of triangular elements which are internally rigid, but can slip relative to each other. In Secs. 2 and 3 we derive the basic equations in the interior and on the boundary based on the Principle of Virtual Work. In doing this, we visualize the edge between two triangles as a rectangle of small thickness and ignore second-order effects. Also, it is shown that we have one degree of freedom per node for this incompressible model. Section 4 considers a simple problem explicitly to point out an interesting aspect of non-uniqueness, and in Sec. 5 we present results for an approximation to the Prandtl problem for a rough punch. The results are compared with known exact and numerical solutions. Finally, some

conclusions are drawn in Sec. 6.

2. Interior domain. Although the theory can be developed for any regular or irregular arrangement of triangles, we shall consider only the case of a regular array of isosceles right triangles illustrated in Fig. 1. In this two-dimensional finite element model the triangles are considered as rigid bodies which can slip relative to each other but must not become separated. Therefore, the only "strains" in the model will be measured by the relative motion or slip between the two adjacent triangles.

Let d_{ij} be the slip along the edge ij joining nodes i and j. It will be taken as positive when, from the viewpoint of an observer at node i and facing edge ij, the triangle on the right moves towards the observer with respect to the triangle on the left. Evidently $d_{ij} = d_{ji}$. A dimensionless strain is then defined by

$$\omega_{ij} = d_{ij}\, \ell_{ij}/\ell_o^2 \qquad (1)$$

where ℓ_{ij} is the length of the edge and ℓ_o is a reference length for the domain.

If we ignore boundary effects, then in a large domain with N nodes, there will be 2N triangles and 3N edges, hence there will be 3N generalized strains. The requirement that triangles do not separate will introduce several compatibility constraints among

these strains. In the first place, there can obviously be no relative rotation of triangles so that at most we need consider only two degrees of translational freedom per triangle, or a total of 4N for the field. However, since even a uniform separation is prohibited, there will be an additional constraint on each of the 3N edges, so that we are left with only N degrees of freedom, i.e. one degree of freedom per node. It follows that, if one elementary mechanism is associated with each node, all possible infinitesimal motions in a large field may be expressed as linear combinations of these mechanisms.

Figure 2 shows the elementary mechanisms associated with generic "small" and "large" nodes. Evidently Fig. 2b may be obtained from Fig. 2a by a change of scale and a rotation so that the mechanisms are essentially the same.

We define generalized displacements by

$$\theta_D = \ell d/\ell_o^2 \qquad \theta_G = \ell d/\ell_o^2 \tag{2}$$

The displacements across AD and DG must be equal so that we can refer directly to the diagonal edge AG in Fig. 2a; the diagonals through G, however, must be considered independently. Evidently the strains associated with the mechanisms in Figs. 2a and 2b respectively are

$$\omega_{FG} = \omega_{GB} = \omega_{BA} = \omega_{AF} = \theta_D$$

$$\omega_{AG} = \omega_{BF} = -2\theta_D \tag{3a}$$

$$\omega_{FL} = \omega_{LH} = \omega_{HB} = \omega_{BF} = \theta_B$$

$$\omega_{FG} = \omega_{LG} = \omega_{HG} = \omega_{BG} = -\theta_B \qquad (3b)$$

The total strain along any edge will be the resultant of several mechanisms. For example

$$\omega_{FG} = \theta_D + \theta_I - \theta_F - \theta_G \qquad (4a)$$

$$\omega_{AG} = \theta_B + \theta_F - 2\theta_D \qquad (4b)$$

Let us expand a generic edge PQ to a finite thickness $\ell_o \delta$ as in Fig. 3. Then the displacement field

$$u = (1/2)(u' + u'') + y\, d_{PQ}/\ell_o\delta \qquad v = v' \qquad (5)$$

is continuous with the rigid triangle motions and the internal strain is the constant

$$\gamma_{xy} = d_{PQ}/\ell_o\delta = \omega_{PQ}\ell_o/\ell_{PQ}\delta \qquad (6)$$

Since a constant strain implies constant stress for any reasonable constitutive behavior, we define a generalized stress for the edge by

$$\tau_{PQ} = \lim_{\delta\to 0} \int_A \frac{\sigma_{xy}\, dA}{k\ell_o\ell_{PQ}\delta} = \frac{\sigma_{xy}}{k} \qquad (7)$$

where k is the yield stress in shear. Then the dimensionless internal work is

$$w_{int} = W_{int}/k\ell_o^2 = \tau_{PQ}\omega_{PQ} \qquad (8)$$

which satisfies Prager's criterion [5] for generalized variables.

No external work will be done during the mechanism motions in Fig. 2, so that the associated internal work must vanish. Thus we obtain the generic

equilibrium equations

$$\tau_{FG} + \tau_{GB} + \tau_{BA} + \tau_{AF} - 2\tau_{AG} - 2\tau_{BF} = 0$$

$$\tau_{FL} + \tau_{LH} + \tau_{HB} + \tau_{BF} - \tau_{FG} - \tau_{LG} - \tau_{HG} - \tau_{BG} = 0 \qquad (9)$$

at small and large nodes, respectively.

Since stress and strain are constant in an edge, the constitutive equations for an elastic/perfectly plastic material may be written as

$$\text{IF } |\tau_{PQ}| < 1 \text{ OR } \tau_{PQ}\dot{\omega}_{PQ} < 0$$

$$\text{THEN } \dot{\tau}_{PQ} = (G'\ell_o/k\ell_{PQ})\dot{\omega}_{PQ} \qquad (10a)$$

$$\text{ELSE } \dot{\tau}_{PQ} = 0 \qquad (10b)$$

where we have defined

$$G' = G/\delta \qquad (11)$$

Equations 10 and 11 imply that the edge is made of a fictitious material whose shear modulus tends to zero with δ so that G' remains finite. For such a model non-zero slips can be found even in the elastic range, but they will be expressed in terms of the single unknowable modulus G'.

3. Boundary value problem. In the previous section we have defined a model with one generalized displacement variable θ_i for each of the N interior nodes. For N sufficiently large, there are approximately N generalized displacements θ_i, 2N generalized strains ω_{ij}, and 2N stresses τ_{ij}. To determine these 5N unknowns, we have 2N strain-displacement equations (3), N equilibrium equations (9), and 2N constitutive equations (10). However, for any finite number N, the number of

variables and equations may vary slightly from these numbers due to some nodes and edges being on the boundaries.

To illustrate, let us regard ACHF in Fig. 2b as a complete domain subject to the indicated boundary conditions. We regard the boundary conditions as being applied to fictitious triangles external to the boundary. For example, triangle E'BC above line BC moves down with a prescribed velocity as indicated in Fig. 4.

No mechanism is associated with the fictitious point E', and the mechanism associated with B (Fig. 4) is simpler than that for an interior node. Therefore, Eq. (4a) should be replaced by

$$\omega_{BC} = \theta_E - (\theta_B + \theta_C)/2 \qquad (12)$$

Next, we observe that in any finite rectangle the total number of degrees of freedom is one less than the total number of nodes. Indeed, if each interior and boundary node is given an equal motion θ, the result in view of (4) and (12) will be to leave the entire domain in its original position. Therefore, we may arbitrarily set $\theta_M = 0$ and eliminate the corresponding equilibrium equation as being a linear combination of the other equilibrium equations.

In the interior of Fig. 2b there are 5 unknown θ_i and 12 unknown ω_{ij} and τ_{ij} with a corresponding 5 equilibrium and 12 constitutive and strain-displacement relations. We now examine each boundary segment to determine the additional unknowns and equations.

The fictitious triangles J'ML and I'LK cannot move vertically, so that $\theta_M = 0$ implies that $\theta_L = 0$ which in turn implies $\theta_K = 0$. The stress $\tau_{LM} = \tau_{KL} = 0$ and the strains are free but of no interest. Thus we have added neither unknowns nor equations to the list of unknowns. Evidently the same conclusion applies to CHM and $\theta_H = \theta_C = 0$.

On KFA, a non-zero normal displacement is prescribed. Since $\theta_K = 0$ it follows from Fig. 4 that

$$\theta_F = 2u_o \ell/\ell_o \qquad \theta_A = 2\theta_F = 4u_o\ell/\ell_o \tag{13}$$

A mechanism motion compatible with (13) leads to the equilibrium equation

$$\tau_{KG} + \tau_{AG} - \tau_{FG} + 2\tau_{FB} = T_2 \tag{14}$$

where T_2 is the average dimensionless normal force on AK. Since $\tau_{KF} = \tau_{FA} = 0$ and the strains are irrelevant, we have added one unknown force T_2 and one new equation to our system.

On the top edge $\tau_{AB} = 0$ and ω_{AB} is irrelevant, but τ_{BC} and ω_{BC} are additional unknowns subject to (10) and (12) (with $\theta_C = 0$). The mechanism at B must satisfy

$$\theta_B = -2v_o\ell/\ell_o \tag{15}$$

and the corresponding equilibrium equation is

$$2(\tau_{AG} + \tau_{GC} - \tau_{BG}) - \tau_{BC} = T_1 \tag{16}$$

where T_1 is the average dimensionless normal force on BC. Therefore, the total system balances with 33 equations and unknowns.

4. Solution. As with most elastic-plastic problems, the general method of solution is to assume that all θ_i, τ_{ij}, and ω_{ij} are known at a generic time t_o, convert all equations to rate form, and solve for $\dot{\theta}_i$, $\dot{\tau}_{ij}$, and $\dot{\omega}_{ij}$, and then find θ_i, τ_{ij}, and ω_{ij} at $t_o + \Delta t$ by linear integration. The interval Δt is chosen so that no edge changes between elastic and plastic during the interval, hence each edge is always on the same branch of (10) during each rate solution.

Problems associated with choice of branch in (10) turn out to be easily handled, but an interesting lack of uniqueness occurs at certain stages. To illustrate this phenomenon let us consider in detail the problem where $v_o = 4d$, $u_o = -d$, and we are not concerned with the resultant forces T_1 and T_2. Then the non-zero boundary rates are

$$\dot{\theta}_B = -4\dot{d} \qquad \dot{\theta}_A = -2\dot{d} \qquad \dot{\theta}_F = -\dot{d} \tag{17}$$

where we have taken $\ell_o = 2\ell$.

There are 5 homogeneous equilibrium rate equations

$$\dot{\tau}_{FG} + \dot{\tau}_{LG} - 2(\dot{\tau}_{KG} + \dot{\tau}_{FL}) = 0 \tag{18a}$$

$$\dot{\tau}_{FG} + \dot{\tau}_{GB} - 2(\dot{\tau}_{FB} + \dot{\tau}_{AG}) = 0 \tag{18b}$$

$$\dot{\tau}_{FL} + \dot{\tau}_{LH} + \dot{\tau}_{HB} + \dot{\tau}_{FB} - (\dot{\tau}_{FG} + \dot{\tau}_{LG} + \dot{\tau}_{HG} + \dot{\tau}_{BG}) = 0 \tag{18c}$$

$$\dot{\tau}_{LG} + \dot{\tau}_{GH} - 2(\dot{\tau}_{LH} + \dot{\tau}_{GM}) = 0 \tag{18d}$$

$$\dot{\tau}_{BG} + \dot{\tau}_{GH} + \dot{\tau}_{BC} - 2(\dot{\tau}_{GC} + \dot{\tau}_{BH}) = 0 \tag{18e}$$

and 13 strain-displacement relations

$$\dot{\omega}_{FL} = -2\dot{\theta}_I + \dot{\theta}_G \qquad \dot{\omega}_{KG} = -2\dot{\theta}_I - \dot{d} \tag{19a,b}$$

$\tau_{ij}\dot{\omega}_{ij} \geq 0$ at a yielding edge. Evidently they will be satisfied for any θ_J satisfying

$$-\dot{d} \leq \dot{\theta}_J \leq 0 \tag{23}$$

so that the kinematic solution is not unique, but it is bounded.

Now, all of the edges involved in a mechanism motion about node J have yielded. Thus, there is no internal work and hence $\dot{\theta}_J$ can not be determined. However, this configuration is not a mechanism since a mechanism motion in either direction would require unloading in some edges. Indeed, if the motion about node J were the only contribution to edges LG and GH for example, $\dot{\theta}_J$ would have to be zero. The freedom allowed by (23) is due to the fact that other mechanisms also produce strain rates and that only the total strain rate is subjected to the inequalities (22).

5. Example. A computer program was written to implement the finite element slip model, and was used to solve the problen illustrated in Fig. 1. An elastic/perfectly plastic material is placed in a perfectly lubricated box and indented with a rigid punch. This problen is a finite domain approximation to the Prandtl problem [1,2] of a rigid rough punch indenting a semi-infinite perfectly-plastic material under conditions of plane strain. It is also essentially the one considered in Sec. 3 except that the domain is larger and $u_o = 0$. Details of the solution and a discussion of the computer program may be found in [6].

The first stage of our solution is the fully elastic range. This stage is terminated when edge pq of Fig. 1 reaches positive yield for $v_o = 2.27\ G'/k$ and an averaged compressive stress under the punch of 2.50, i.e., $T_1 = -2.50$. Figure 5 pictures the elastic displacement field by showing the averaged vertex displacements at representative small nodes.

As v_o is increased above its maximum elastic value there will be a succession of elastic-plastic stages. The sequence in which edges become plastic is indicated in Fig. 6, and the load-deflection curve for the punch is shown in Fig. 7.

No difficulties with the solution are encountered until stage 10. The first rate solution at this stage shows that edge pv which reached positive yield at the end of stage 6, now has a negative strain rate $\dot{\omega}_{pv}$ and violates the inequality of the constitutive equation (10). Therefore, this rate solution must be rejected and edge pv assumed to be elastic again for stage 10. It remains elastic during all subsequent stages. The maximum unloading occurs at the end of stage 15 and is about 2% less than the yield stress.

Edge hi alternates being elastic and plastic. At the end of stage 10 this edge reaches positive yield and remains at yield until the beginning of stage 15. It is elastic in stages 15 and 16, plastic in 17, elastic again in stages 18-21, and plastic from then on. After initial yield, the elastic stress is never less than 99% of the yield stress so that, in fact, no serious error would be introduced if unloading were

neglected.

At the end of stage 19 we see in Fig. 6 that the edges of the elementary large node mechanism of node p are all at yield. Therefore, $\dot{\theta}_p$ is undetermined, subject to the inequalities of Eq. (10). These inequalities reduce to

$$-.179\dot{v}_0 \geq \dot{\theta}_p \geq -.189\dot{v}_0 \tag{24}$$

for stages 20 and 21.

Fig. 6 also shows that at the end of stage 21 all of the edges associated with the elementary mechanism of small node k are also at yield so that there is a further singularity in the stiffness matrix. The rate solution for stage 22 puts the following bounds on $\dot{\theta}_k$ and $\dot{\theta}_p$:

$$\begin{aligned} -.114\dot{v}_0 &\geq \dot{\theta}_k \geq -.121\dot{v}_0 \\ .055\dot{v}_0 + 2\dot{\theta}_k &\leq \dot{\theta}_p \leq -.190\dot{v}_0 \end{aligned} \tag{25}$$

At the end of stage 22, four edges simultaneously reach yield, $T_1 = -6.00$, and $v_0 = 25.05$ G'/k. It is evident from Fig. 6 that sufficient edges have yielded to permit the mechanism motions shown in Fig. 8a with all inequalities in (10) being satisfied, as well as numerous other mechanisms. Since all stresses in the non-homogeneous equilibrium equation corresponding to (16) are at yield and hence constant, the load is constant, and $T_1 = -6.00$ represents the yield-point load.

In order to evaluate this method of velocity-discontinuities we compare the results in the fully

elastic range and at the limit load condition with analytical and other numerical results.

Green and Zerna [7] have obtained an analytical solution to the Prandtl problem for an incompressible elastic material. Their displacements are shown by dashed arrows in Fig. 5. The dotted arrows show the solution of the elastic problem according to the classical finite element model with constant-strain triangles and no slip, taking $\nu = 0.49$.

Figure 5 shows surprisingly good agreement for the elastic solution. It must, of course, be emphasized that the dimensionless displacements for the other solutions are defined in terms of known physical constants, whereas the slip model they include the essentially unknowable modulus G'. However, by choosing the constant G' = 14.05 G so that the overall slopes match in Fig. 7, we obtain good agreement over the entire field.

The agreement of the three solutions is quite good near the punch and along most of the free boundary. The poor agreement along the edges suggests that the size of the box in the model was too small to give a good approximation to a semi-infinite domain.

Little information is available for comparison of the various elastic-plastic stages, but a partial solution at the yield-point load was first given by

Prandtl [4] and was later shown by Shield and Drucker to be complete [8]. Fig. 8b shows the resulting kinematic pattern. The yield point stress is:

$$T_1 = - (2 + \pi) = - 5.14 \qquad (26)$$

compared with our value of -6.00.

6. Conclusions. Other examples have been considered in [6]. These include the Prandtl problem for a smooth punch, and tension of bars with a deep perpendicular slit in either or both sides. The results are all generally similar to the problem of Sec. 5. In all cases, the program ran smoothly and the difficulties posed by unloading and by non-unique velocity solutions proved easily surmountable.

We have presented a model based on slip which is easily adapted to computer use and which appears to give reasonable results for an elastic/perfectly-plastic material. Potential difficulties caused by a partial lack of uniqueness prior to yielding do not prove unsurmountable, although it would be desirable to further investigate this phenomenon. The fact that G' cannot be determined means that only relative displacements can be determined, but it does not affect the stress solution and appears a small price to pay for the simplicity of the model.

An obvious question arises as to the feasibility and desirability of a model which would include both constant-strain deformations of the triangles and slip between them. It turns out that such a combined model separates into two problems corresponding to its two

constituients, and that the two problems are only weakly coupled. Details of this combined model are reported an elsewhere [6].

References

1. Turner, M.J., Clough, R.W., Martin, H.C., and Topp, L.J., "Stiffness and Deflection Analysis of Complex Structures," J. Aero. Sci.,Vol. 23, 1956, pp. 805-823.
2. Prager, W. and Hodge, P.G., Jr., Theory of Perfectly Plastic Solids, J. Wiley and Sons, Inc., New York, 1951.
3. Nagtegaal, J.C., Parks, D.M. and Rice, J.R., "On Numerical Accurate Finite Element Solutions in the Fully Plastic Range," Comp. Meth. Appl. Mech. & Eng., Vol. 4, 1974, pp. 153-177.
4. Prandtl, L., "Ueber die Haerte plasticher Koerper," Goettinger Nachr., math-phys. Kl, Vol. 1920, 1920, pp. 74-85.
5. Prager, W., "The General Theory of Limit Design," Proc. 8th International Congress of Applied Mechanics, Vol. 2 (Istambal 1952), 1956, pp. 65-72.
6. Van Rij, H., PhD Dissertation, University of Minnesota, 1978.
7. Green, A.E. and Zerna, Theoretical Elasticity, Oxford: Claredon Press, 1954.
8. Shield, R.T., and Drucker, D.C., "The Application of Limit Analysis to Punch Indentation Problems," J. Appl. Mech., Vol. 20, 1953, pp. 453-460.

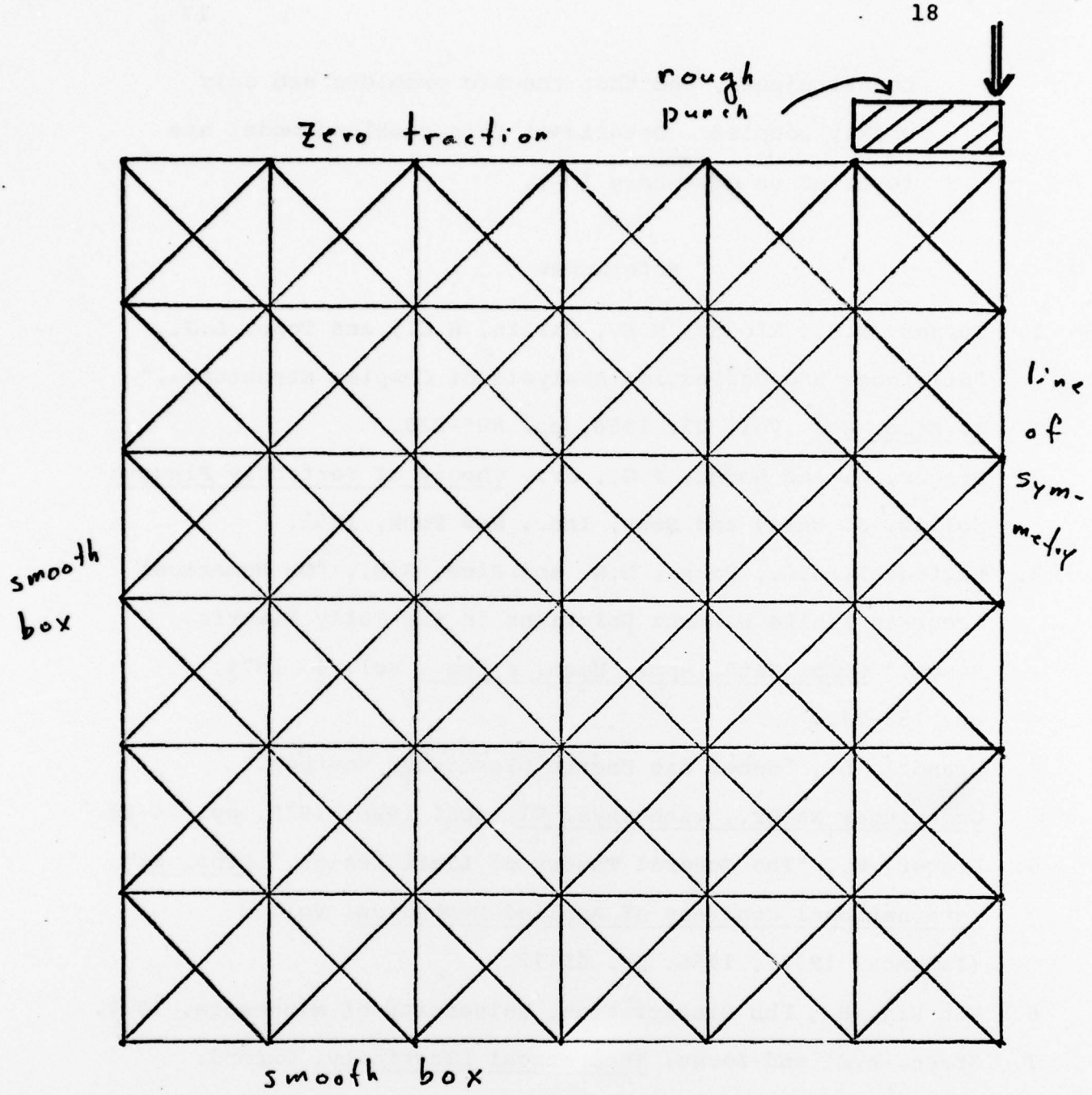

Fig. 1 Prandtl punch problem

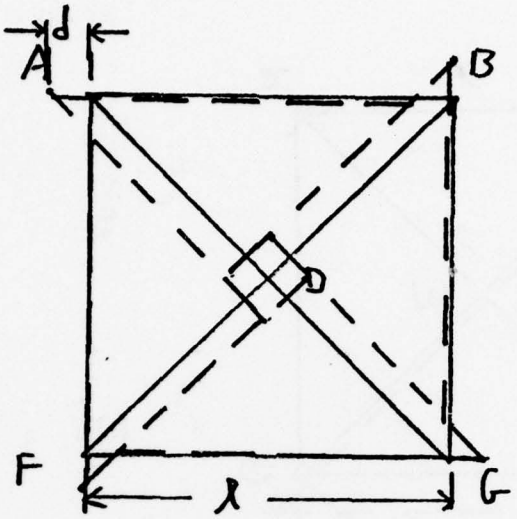

(a)

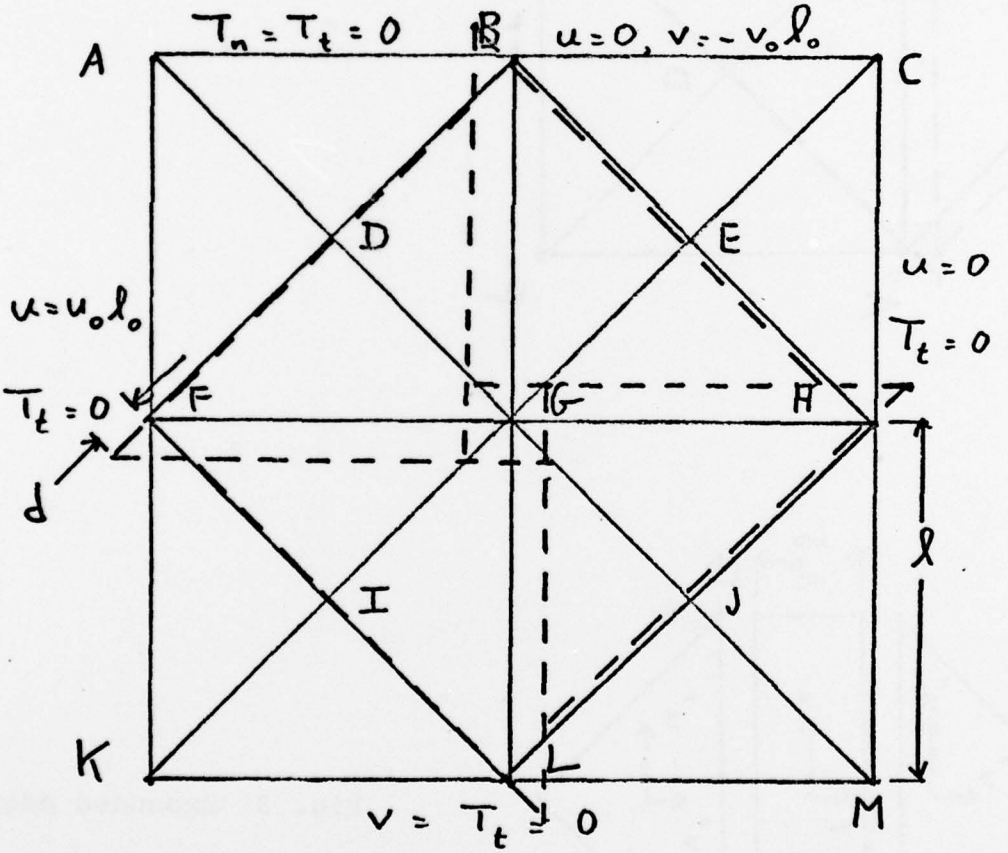

(b)

Fig. 2 Elementary mechanisms (a) small node (b) large node

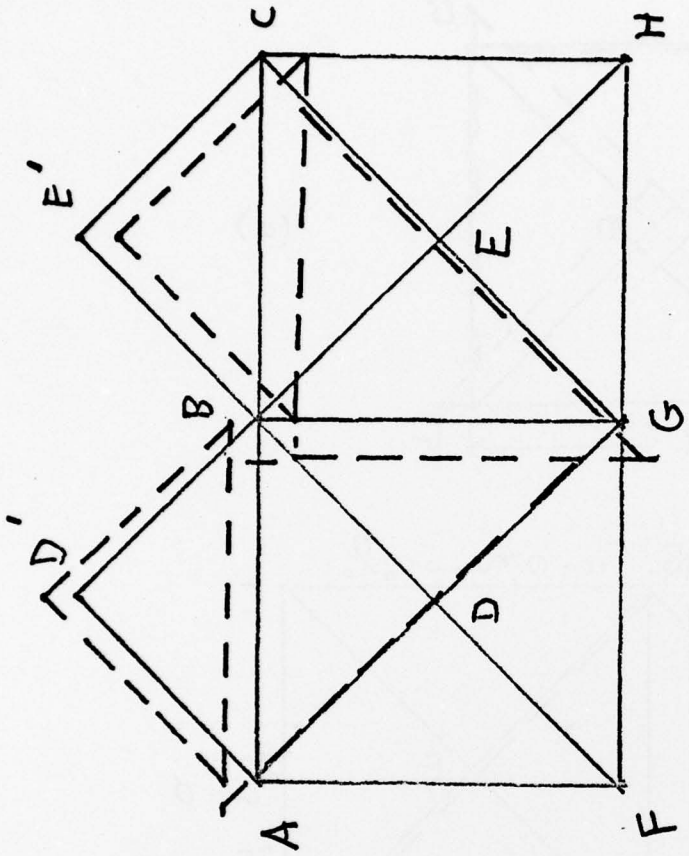

Fig. 4 Boundary mechanism

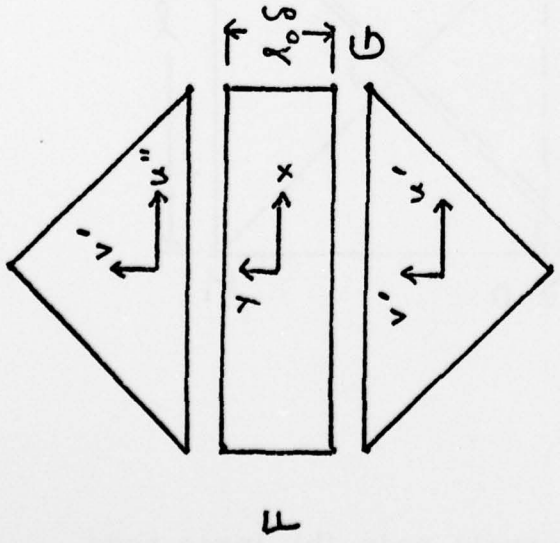

Fig. 3 Expanded edge

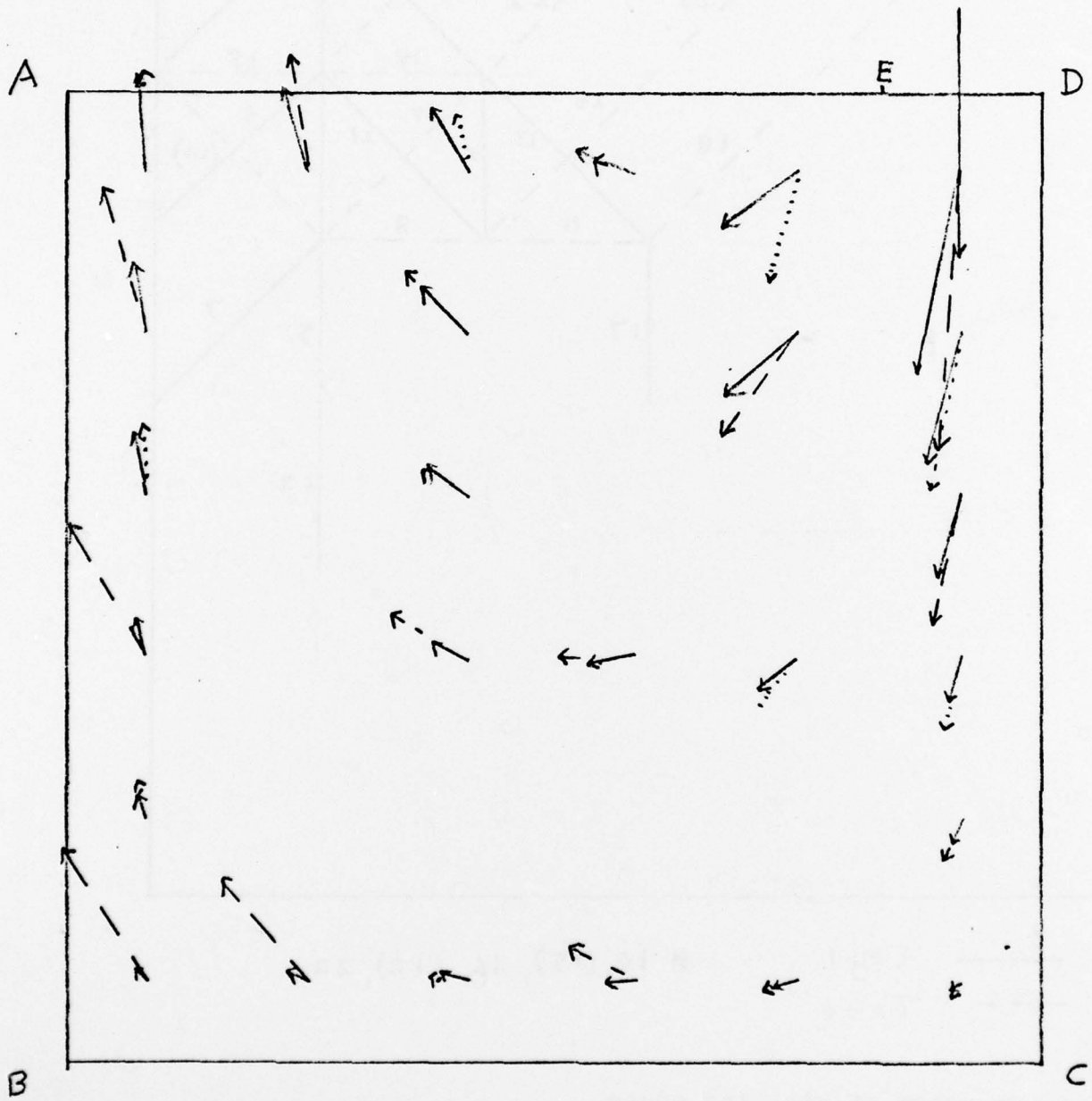

——————→ slip model

— — — → analytical solution [7]

. . . . . → classical model

Fig. 5 Elastic displacements

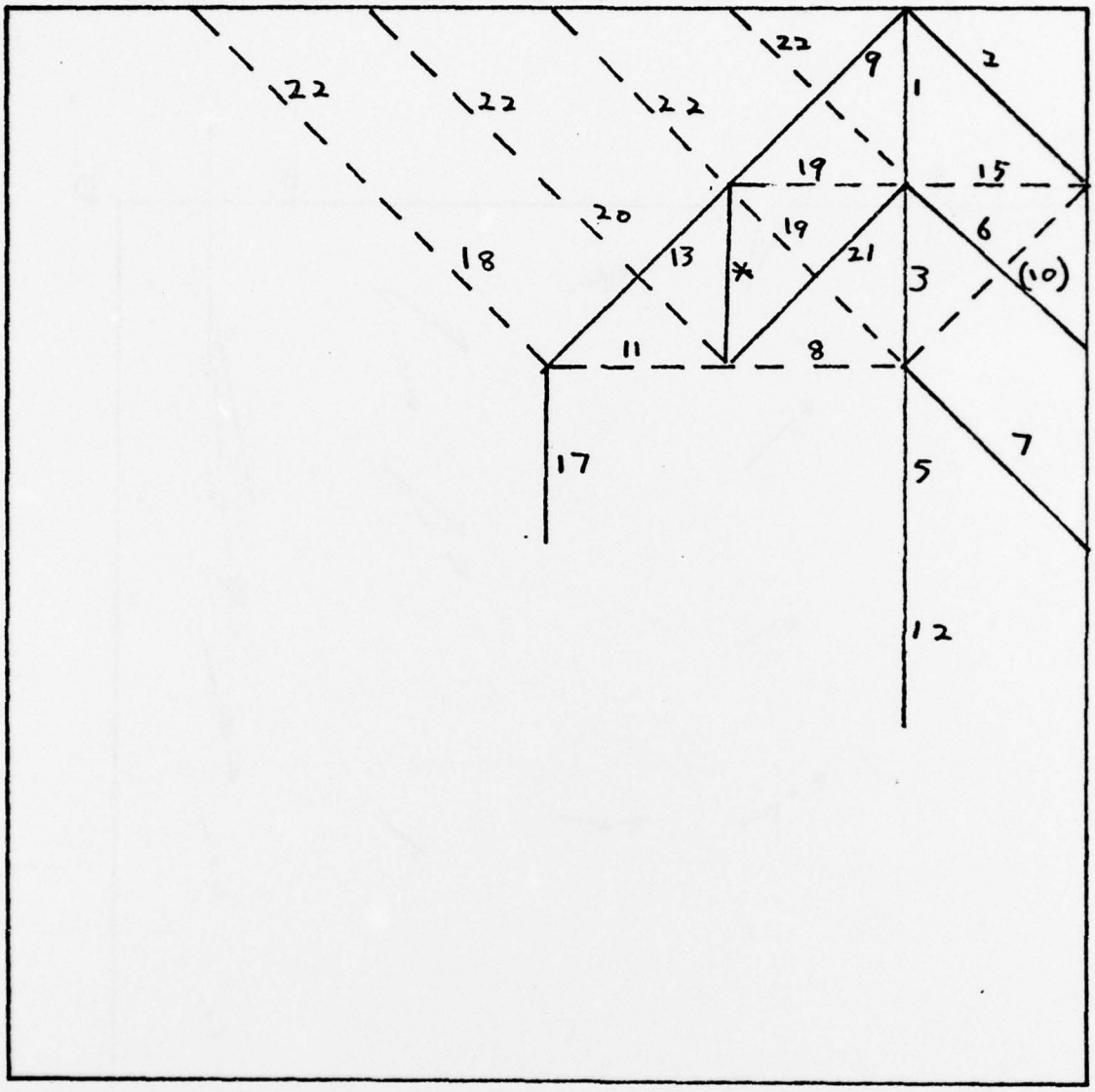

Fig. 6 Sequence of yielding edges

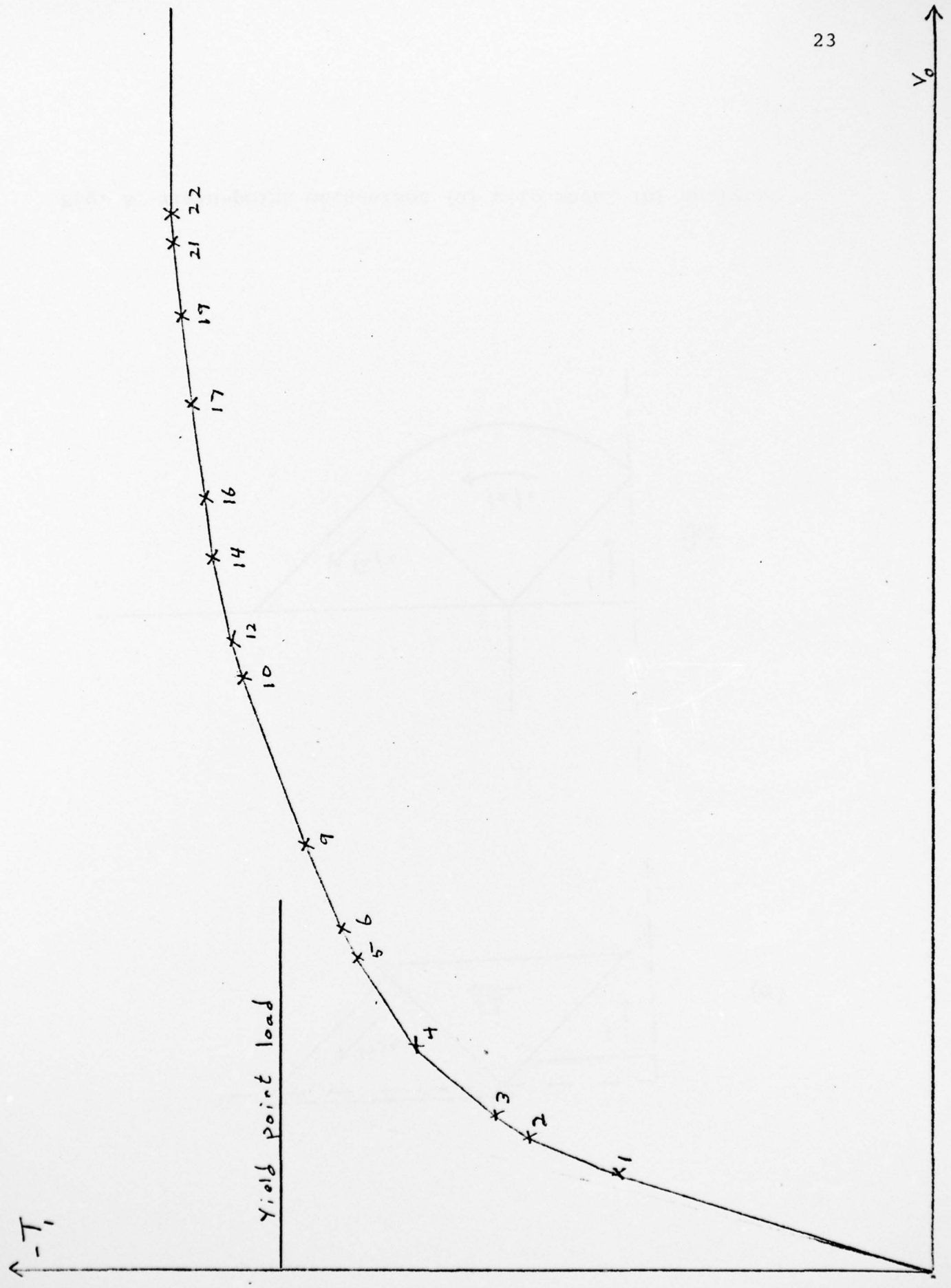

Fig. 7 Load-displacement curve

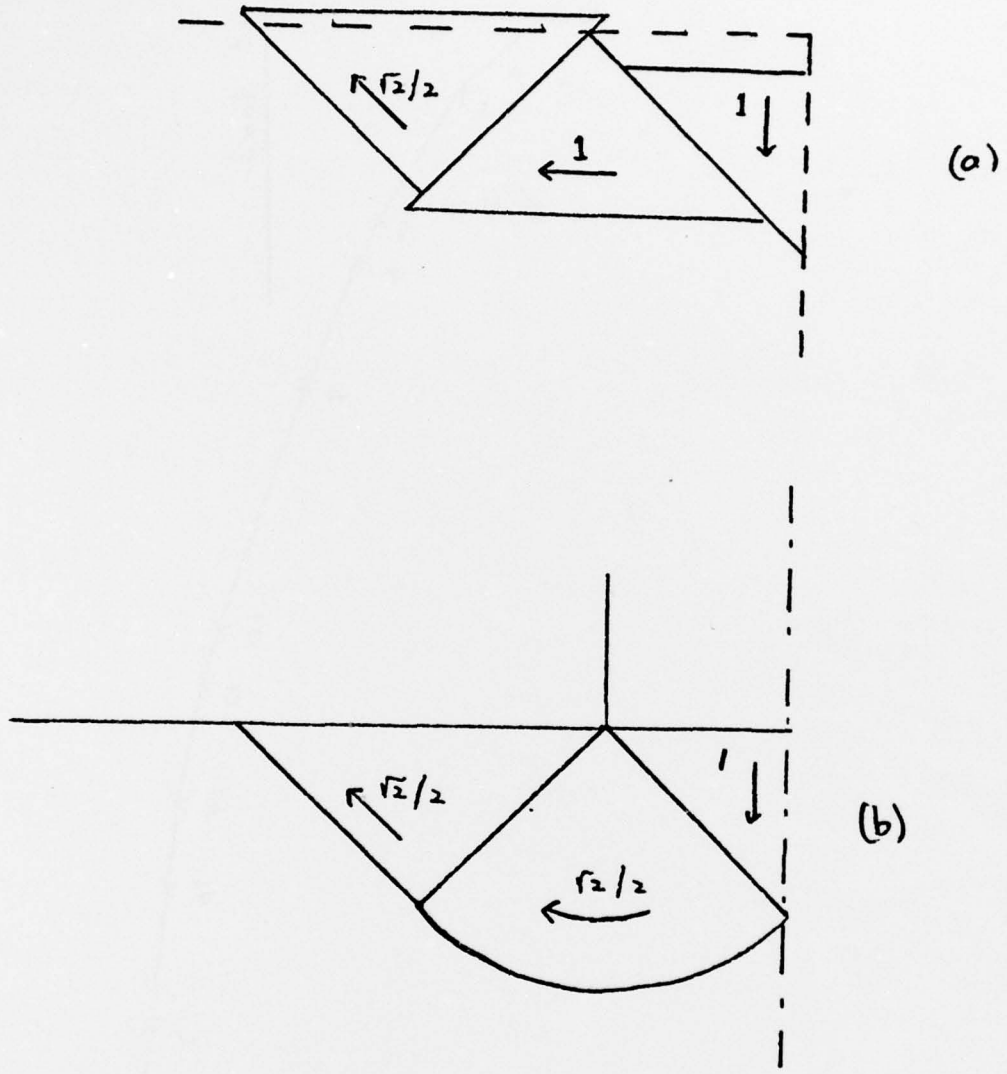

Fig. 8 Yield-point mechanisms (a) slip model (b) analytic